Appl. Phys. B 70 [Suppl.], S155–S160 (2000) / Digital Object Identifier (DOI) 10.1007/s003400000329

Applied Physics B
Lasers
and Optics

Invited paper

Production of $> 10^{21}$ W/cm^2 from a large-aperture Ti:sapphire laser system

J.D. Bonlie, F. Patterson, D. Price, B. White, P. Springer

Lawrence Livermore National Laboratory, P.O. Box 808, m/s L-251, Livermore, CA 94550, USA

Received: 7 October 1999/Revised version: 10 March 2000/Published online: 24 May 2000 –

Abstract. We have successfully developed a laser system to produce pulses with a wavelength centered at 800 nm, energies above 15 J, temporally compressed to 75 fs and focused to power densities beyond 10^{21} W/cm^2. Enabling technologies include chirped-pulse amplification (CPA), 10 cm aperture Ti:Al_2O_3 crystals, large diffraction gratings, and an energetic Nd:glass laser for pumping the final two amplifiers. Measurements of the compressed pulse spectrum, frequency resolved optical gating (FROG) diagnostic, and focal spot are presented. We have also investigated and developed a technique for suppression of transverse parasitic lasing in large-aperture Ti:sapphire crystal amplifiers.

PACS: 42.65.Re; 52.40.Nk; 41.85.Ew

The principal activity of our research group at Lawrence Livermore National Laboratory (LLNL) is directed at the study of high-energy-density matter with an emphasis on equation of state and opacity. The use of ultra-short-pulse laser-matter interactions can provide a new technique for the creation of high-energy-density plasmas in the laboratory. Our efforts are differentiated from other LLNL laser facilities in that we utilize prepulse clean 50 to 150 fs laser pulses to deposit energy in solid density matter prior to the plasma expansion. To further this research, we have developed a novel short-pulse laser capable of focal intensities in excess of 10^{21} W/cm^2 with energies on target in escess of 15 J. We refer to the laser system as "JanUSP", so named since we are using one arm of our "Janus" Nd:glass laser system as a pump source for the final two stages of an ultra-short-pulse (USP) laser system.

This system was conceived more than seven years ago and takes advantage of several technological advancements developed since then. While waiting for the development of suitable optical components, we experimented with a smaller-scale CPA system and various final amplifier schemes, including flashlamp-pumped Ti:sapphire [1] and Nd:glass laser-pumped Ti:sapphire [2, 3]. The latter of these schemes has been in use at our USP laser facility for over four years and has proven to be a robust source for the generation of power densities $> 10^{19}$ W/cm^2.

Chirped-pulse amplification laser systems have extensively evolved and matured since the mid-1980s. The two gain media most commonly employed for CPA are Nd:glass and Ti:sapphire. Recently, the scaling of a CPA Nd:glass system to very high intensity ($\approx 2 \times 10^{20}$ W/cm^2) has been achieved with large-aperture disk amplifiers (46 cm diameter) on the Petawatt Laser Project at LLNL [4]. Many factors must be considered when selecting laser amplifier media. Generally speaking, when comparing Ti:sapphire to Nd:glass, the gain bandwidth of Ti:sapphire is more than 10 times that of Nd:glass; saturation fluence (E_s) is ≈ 1 J/cm^2 for Ti:sapphire and ≈ 5 J/cm^2 for Nd:glass [5], and the small-signal power gain coefficient(g_0) is much greater for Ti:sapphire. Until now, efforts to scale titanium-based laser systems to intensities greater than 10^{19} W/cm^2 have concentrated on reducing the amplified pulsewidth to less than 20 fs [6, 7], because significantly higher pulse energies have been limited by the availability of large-aperture crystals with high optical quality. Here, we report on a CPA laser system which utilizes the largest Ti:sapphire disk amplifiers ever produced (10 cm diameter). Optimization of disk amplifiers with larger aspect ratios (transverse to longitudinal) and increased pump energy, becomes increasingly difficult as suppression of parasitic lasing becomes a key challenge.

Ti:sapphire amplifiers are typically longitudinally pumped by Q-switched neodymium oscillators frequency doubled to ≈ 530 nm, which is near the titanium absorption peak. Larger pump sources append flashlamp-pumped Nd:glass amplifiers to the oscillator before frequency doubling. Beam profiles from Ti:sapphire amplifier stages can also be effectively shaped by adjusting the size, position and profile of the pumping beams; however, poorly shaped pump profiles can deleteriously affect the disk amplifier's spatial gain uniformity.

Correspondence to: J.D. Bonlie (E-mail: jbonlie@genoacorp.com) or D. Price (E-mail: price4@llnl.gov, Fax: 925-422-2253)

1 System configuration

Our laser is very similar to what we have previously described [2, 3], where as much as 3 J of chirped-pulse energy has been obtained from a 3 cm aperture Ti:sapphire amplifier longitudinally pumped with 15 J of 532 nm light. The laser system described here is a completely separate facility but similar up to the 3 cm aperture amplifier stage. From this point the 280 mJ chirped pulse then double-passes each of the final two Ti:sapphire amplifiers in "V" configurations. The beam then enters a vacuum compressor and is routed to the target chamber and focused with an off-axis parabolic (OAP) mirror. Only reflective optics are used once pulse recompression is begun.

2 Component and layout discussion

We have been able to bring together three important enabling technologies: (1) an energetic, large-aperture laser pump source (for the Janus laser is capable of supplying over 150 J of 532 nm light); (2) large high-quality diffraction gratings; (3) large-aperture laser-grade Ti:sapphire crystals for amplification.

A significant amount of effort was put in to optimize one arm of LLNL's Janus silicate glass laser system in order to use it for pumping the final two Ti:sapphire amplifiers. For the front end of this source we selected a Quanta Ray GCR-11 seeded Nd:YAG laser. This source has enabled many system improvements. The 8 ns temporal profile (reduced to ≈ 6 ns after amplification; and ≈ 5 ns after doubling) is well-suited to our 17 mm KDP doubling crystals and, by starting with an energetic ≈ 60 mJ pulse, we were able to remove several amplifiers and optics from the original chain, resulting in a much lower B-integral (integrated nonlinear phase due to intensity propagation effects [8]) and improved spatial characteristics. Alignment is much easier with this 10 Hz source as there is even enough light through the chain to see the 532 nm beam on the final Ti:sapphire amplification table. The improved spatial profile is flat to within 20% after being doubled to 532 nm. Amplification of the 1ω pulses to more than 300 J in a 9 cm diameter beam has been achieved with no degradation to the laser optics. Nd:glass amplifier technology is well-established and highly reliable. Disadvantages of using Nd:glass amplifiers in the pump chain include their physically large size and having to operate them at low repetition rates due to thermal issues. The repetition rate for our system is 10 Hz, with the exception of the final two amplifier stages where the maximum rate is limited to 3 shots per hour by the glass amplifiers.

Routinely, 240 J of 1ω pulses is doubled to ≈ 120 J of 532 nm light and then relay-imaged using two ($F = 7.5$ m) lenses and a vacuum tube into the USP lab, where it is then beam-split and sized using lenses to the appropriate diameters for longitudinal pumping the final two Ti:sapphire amplifiers. Accounting for some losses in pump path, the 3-cm-diameter Ti:sapphire amplifier is pumped on each side with ≈ 9 J and the final amplifier with ≈ 40 J at 9 cm diameter on each side. The design of the amplifier layout also took into consideration the timing of the pump arrival to the arrival of the chirped short pulse. Prior to solving parasitic lasing problems, small amounts of timing jitter resulted in large gain variations in these final amplifiers.

Since an unclipped Gaussian beam is propagated through the amplifier chain, relay imaging is not necessary to prevent diffraction ripple growth as in the case of a top-hat beam (e.g., the NOVA laser). Also, since the quality of the optical components is high and there are relatively few of them, no vacuum spatial filters are needed. Hence, Galilean beam expanders are used between amplifier stages and between the final amplifier and the compressor in the Ti:sapphire chain. The optical paths are sufficiently short that the use of relay imaging in a vacuum is not required. The use of Galilean beam expanders has the added advantage that spherical aberration can be minimized in a properly designed system. We have used ZEMAX optical design software from Focus Software, Inc. to determine the optimum expander design.

If the accumulated B-integral in a laser system approaches 2 radians, the concentration of energy in the focal spot is reduced, with a corresponding drop in total intensity on target. Total calculated B-integral for our system is ≈ 0.51 radians. We estimate that a glass amplifier with the same fluence and achieving the same gain would have five times the accumulated B-integral. Key to maintaining a low B-integral in our system is the use of large-aperture optics at low fluence and high gain amplifiers, few in number, which do not push the extraction efficiency at the expense of the B-integral.

Stretched pulses with energies above 21 J and centered at 800 nm have been measured just in front of the vacuum compressor. The compressor utilizes 1480 l/mm gold coated holographic gratings [9, 10] (G1 = 33 cm diameter, G2 = 40 cm diameter) manufactured at LLNL, and it has an overall throughput efficiency of 75% in double pass. We have found the damage threshold of gratings made with a similar process to be $\geq 200\,\mathrm{mJ/cm^2}$. Initially, a tightly focused spot was difficult to obtain because of the grating mounts that distorted the first-order diffracted wavefront. This situation has been corrected by changing the mounting scheme. Although not always possible, the wavefront of each mounted optical component should be measured in situ. Large optics, in particular, suffer distortions simply due to their weight not being uniformly supported. Temperature variations can also produce stress and induce distortions.

After the pulse is compressed, it is routed to the target chamber (in the same 10^{-5} Torr range vacuum environment), where it is reflected off of a 15.24 cm diameter gold-coated $F/2$ OAP mirror. The beam path through the compressor and onto the OAP has a clear aperture of 15 cm. We have designed an equivalent plane focal diagnostic utilizing an uncoated OAP identical to that used in the target chamber. Transmitted light from one of the final dielectric turning mirrors in the compressor vessel is collected, reflected off two uncoated surfaces, attenuated by $\approx 10^3$ using filter glass, and then focused. The focal point is imaged, using a $60\times$ microscope objective and extension tubes onto a CCD camera, enabling a digitized image resolution of 0.26 μm/pixel. A similar imaging camera is placed in the target chamber and used for cross-checking when optimizing the OAP for minimal astigmatism. The imaging system's spatial calibrations are performed using a Newport RES-1 resolution test target.

2.1 *Parasitic lasing*

Parasitic lasing is among the most important laser physics issues which must be addressed when designing large-aperture high-gain amplifiers. This problem was originally identified and studied in the mid-1960s for ruby lasers [11] and later in the 1970s for large-aperture Nd:glass disk amplifiers [12–15]. Parasitic lasing is due to the formation of a laser cavity by Fresnel reflections at the material interfaces of the gain medium. In general, many complex cavity configurations with multiple reflected ray pathways can simultaneously lase. In Nd:glass disks without special edge claddings, the magnitude of the Fresnel reflections are of the order of $\approx 5\%$ and so the onset of parasitic lasing typically becomes problematic when the transverse gain approaches e^3 (≈ 20) [12]. Above the parasitic lasing threshold, the gain is clamped and no additional energy may be stored in the amplifier. Fortunately for Nd:glass, many suitable materials are available for index matching around $n = 1.5$ and parasitics have successfully been suppressed in disks greater than 30 cm in diameter [14, 15]. The significantly higher index of Ti:sapphire ($n = 1.76$) and its enormous transverse gain (in part due to the longitudinal pumping geometry) present special problems for parasitic suppression techniques [16].

Measurements of parasitic lasing have been performed on three different Ti:sapphire disk amplifiers [17]. Two of the disks (designated as CS1 and CS2) were grown by Crystal Systems, Inc. using the heat exchanger method. These disks are 10 cm in diameter with frosted, roughened edges. The CS1 disk is 1.15 cm long and has single-layer MgF_2 anti-reflection coatings centered at 800 nm (the residual reflectivity (R) at 800 nm being $\approx 1\%$ and that at 532 nm being $\approx 7\%$). The 532 nm absorption coefficient (α) for CS1 is $\approx 1.87\,\mathrm{cm}^{-1}$. In contrast, disk CS2 is uncoated ($R \approx 7\%$ at both 532 nm and 800 nm), has a significantly lower titanium concentration ($\alpha \approx 0.85\,\mathrm{cm}^{-1}$) and a longer length ($L$) = 3.3 cm). The third Ti:sapphire disk studied here, designated UC1, was grown by Union Carbide utilizing the Czochralski method. Disk UC1 has single-layer MgF_2 coatings, a diameter of 8 cm, a length of 2.5 cm and $\alpha \approx 1.8\,\mathrm{cm}^{-1}$. Additionally, our observations indicate that large-aperture Ti:sapphire crystals grown by the heat exchanger method have a much better transmitted wavefront compared with the one using the Czochralski method, and this appears primarily due to the seeding process.

Figure 1 shows the transverse optical power spectrum of crystal CS1 at high pump fluence ($\approx 1.7\,\mathrm{J/cm}^2$). Trace 1 in the figure indicates that the crystal is lasing in the transverse direction; the spectrum has red-shifted and narrowed compared with a series of transverse spectra (not shown) recorded at lower pump fluences (as low as $\approx 0.2\,\mathrm{J/cm}^2$). The onset of transverse lasing in this crystal can also be detected in the time domain. Figure 2, Trace 1 shows the photodiode signal recorded for the double-pass diode laser at the same fluence as Fig. 1. The flat baseline, which is present before the green pump pulse arrives (≈ 0–10 ns), serves as an automatic calibration for the gain measurement since the propagation losses are included (i.e., by definition the net gain = 1 before arrival of the pump pulse). As the green pump pulse is absorbed by the Ti:sapphire disk, the gain rises as the integral of the pulse energy until the transverse lasing threshold is reached, whereupon the gain is rapidly depleted as the inversion is dumped

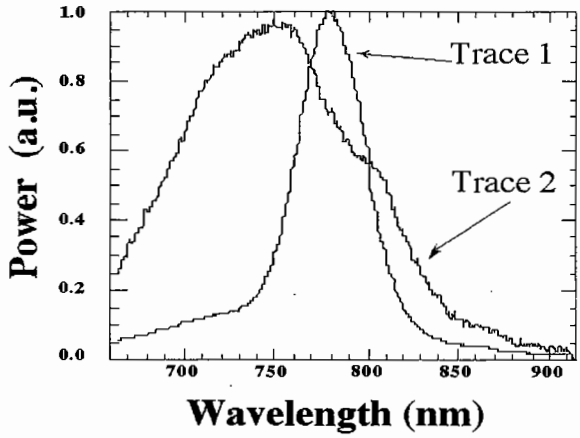

Fig. 1. Transverse spectra of crystal CS1 at high pump power. Trace 1, without cladding; trace 2, with cladding

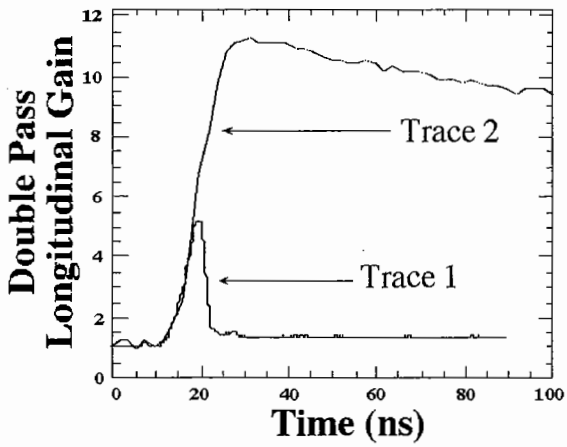

Fig. 2. Oscilloscope record of the double-passed diode laser at the same fluence as Fig. 1

by the lasing modes. The temporal dependence of the transient gain feature in Trace 1, Fig. 2, is consistent with that expected for a gain-switched Ti:sapphire laser with a cavity length (≈ 1.2 ns) and loss ($\approx 99\%$) predicted for the transverse lasing geometry of the CS1 disk. After the transverse lasing modes drop below-threshold, a small residual longitudinal gain remains and persists for several microseconds (consistent with the Ti:sapphire lifetime). Close examination of a series of spectra and scope traces indicates that the threshold for transverse lasing occurs at $\approx 0.7\,\mathrm{J/cm}^2$.

We have explored techniques for suppression of the transverse lasing. Simple application of black ink to the frosted edges of the crystal yielded only a minor increase in the lasing threshold. Cladding the CS1 crystal with an index-matched thermoplastic polymer (R.P. Cargille Laboratories, catalog number 24170) doped with an absorber (powdered ink from a Canon toner cartridge, catalog number F41-9502-740) produced much more significant results. For 800 nm light, the thermoplastic is highly transmissive and has an index of refraction (n) of 1.6849. The Fresnel reflection at the Ti:sapphire interface ($n \approx 1.76$) is thus estimated to be $\approx 0.048\%$, which implies that transverse parasitic lasing should not occur across the input face until the transverse gain is ≈ 2100.

Figures 1 and 2 also show the spectral and temporal characteristics for the cladded CS1 crystal. Trace 2 in Fig. 1 shows a transverse fluorescence spectrum with a center wavelength and bandwidth typical for below threshold optically pumped Ti:sapphire crystals [18]. Trace 2 in Fig. 2 shows the temporal dependence of the double-passed diode laser through the cladded CS1 crystal. In contrast to Trace 1 in the figure, where a short gain-switched pulse indicative of parasitic transverse lasing is observed, Trace 2 shows a reduced fluorescence lifetime (400 ns) but no evidence for transverse lasing.

Recently, we have had the frosted perimeter of CS2 ground and polished (non-optically) at a dual bevel (3° and 4°), extending from the center to the crystal faces. Then the perimeter is encased with the thermoplastic solution. No parasitic lasing has been observed with 120 J of 532 nm pump in a 9 cm diameter beam.

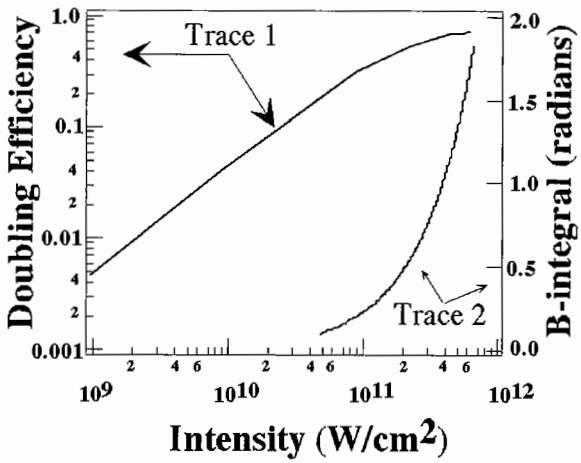

Fig. 3. Calculated values versus intensity for a 0.8-mm-thick KDP crystal using an 80 fs pulse. Trace 1, doubling efficiency, trace 2, worst case B-integral contribution from the crystal

3 Discussion of prepulses

Prepulse is an undesirable parasite common in femtosecond laser systems. For many applications the contrast of prepulse to main pulse intensity is not an issue; however, for solid density plasma studies, prepulse will directly affect the density conditions when a short-duration high-energy pulse arrives. The main sources of prepulse are: (1) pulses leaking from previous round trips in the regenerative amplifier; (2) ASE–with contributions from each stage of amplification but dominated by contributions from the regenerative amplifier; (3) high-order phase distortions, typically due to system bandwidth limitations and/or stretching or compression errors. We strive for a focused prepulse with power density no greater than 10^{11} W/cm^2.

We have been working to minimize prepulse on several fronts. The prepulse due to previous round trips in the regenerative amplifier can be effectively attenuated providing a contrast of 1:10^9 with two stages of good-quality crossed-glan laser polarizers and Pockels cells after the regenerative amplifier. Our system uses one of these stages after the five-pass bow-tie amp, which also helps to attenuate ASE accumulations up to that point. Large-aperture Pockels cells do not turn on quickly enough to effectively attenuate ASE in the nanosecond range just prior to the main pulse. That is why we plan to amplify the oscillator pulses with an additional multipass Ti:Sapphire stage, and then propagate this through a saturable absorber and pulse stretcher so that the regenerative amplifier is more energetically seeded [19]. This should improve contrast by at least 100 times from the measured ASE intensity contrast of 5×10^7.

Another approach to prepulse cleanup is to place in the setup a frequency-doubling crystal after the compressor. Using the SNLO nonlinear optics code available from A.V. Smith, SNL, Albuquerque, NM, we have estimated that a 10^4 improvement in contrast could be realized with acceptably low levels of temporal pulse broadening and spectral shaping due to group velocity dispersion. Additional calculations have helped us determine 0.8 mm as a practical thickness for the 15-cm-diameter doubling crystal, balancing the practicality of manufacturing with high doubling efficiency over a range of input intensities with

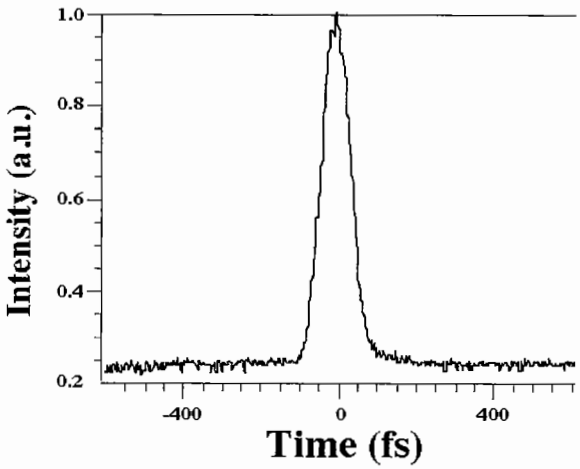

Fig. 4. Temporal lineout from a FROG image of a 15 J compressed pulse. FWHM width = 106 fs, corresponding to a pulsewidth of ≈ 75 fs assuming a Gaussian pulse shape

a low level of pulse distortion and B-integral. Calculations indicate that B-integral will limit the maximum operating fluence and total input energy to about 6 J, as shown in Fig. 3. Ideally, with ≈ 4 J in the second harmonic of the crystal and a 2 μm focal spot diameter, 10^{21} W/cm^2 is still attainable.

The final aspect of prepulse that we address is higher-order phase. An adjustable air-spaced doublet [20, 21] located in our stretcher provides control over second-, third- and fourth-order phase. However the temporal pulse width or spectral phase remains difficult to measure with the high dynamic range desired ($> 10^9$) at the low shot rates required for the full-energy operation of our laser. Our best tool is the standard polarization gate FROG technique [22] but the dynamic range is limited to $\leq 10^3$. Figure 4 shows a lineout of a FROG trace in the temporal direction, indicating a 75 fs FWHM. Our compressor was designed with sufficient bandwidth for 30 fs pulses with spectral clip-points supporting 69 nm of bandwidth for a 15 cm beam.

We currently limit our operations to between 75 fs and 100 fs for several reasons. The primary reason is that the temporal wings of the main pulse become increasingly sensitive to spectral phase distortions as the bandwidth is increased, requiring more emphasis on shot-to-shot stability, and careful control and measurement of the spectral phase to ensure low prepulse levels. Secondly, modifications are required to our existing oscillator and stretcher to accept the full bandwidth of a 30 fs pulse.

4 Results

Figure 5 shows the spectrum of the 15 J compressed pulse. The full-width half-maximum (FWHM) spectral width is about 13.6 nm, nearly identical to that of the mode-locked oscillator pulse. Assuming a Gaussian temporal pulse shape the deconvolved pulsewidth is ≈ 75 fs, giving a time–bandwidth product of ≈ 0.478, which is about 1.1 times the transform limit. Figure 6 is a 1D profile of the focal spot of the low-energy compressed pulse (attenuated from 280 mJ input) using an $F/2$ OAP. We have carefully measured the focal spot through the system at the 280 mJ input level and have found the FWHM to be $2.0 \times 1.6\,\mu$m, or about $1.5\times$ the diffraction limit. We do not expect significant change in the spot dimensions at the 15 J level, since activation of the final two amplifiers only results in an increase of 0.2 rad (calculated) in the B-integral and pump fluences that are similar to those on our other system [2, 3] where we have characterized the focal spot with and without final amplifier pumping. When we estimated the percentage of total energy in the focal spot, we integrated the base of the entire image, which was 120×120 pixels (31.2 microns on a side) digitized to 8 bits, and added 1 bit per pixel–which is the worst case–and still deduced that at least 56% of the energy remains within the spot, supporting our contention that the power density is more than 10^{21} W/cm^2.

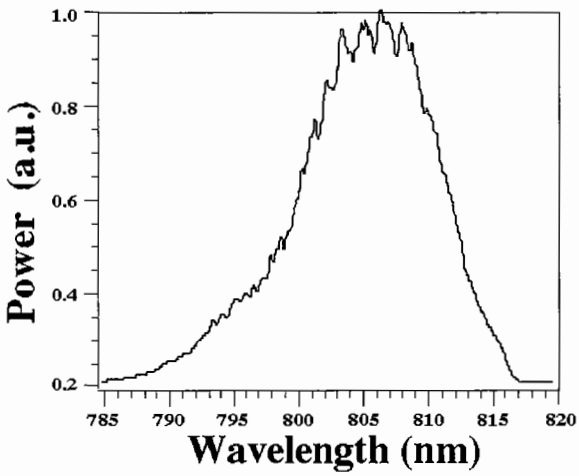

Fig. 5. Power spectrum of the 15 J compressed pulse. FWHM spectral width = 13.6 nm

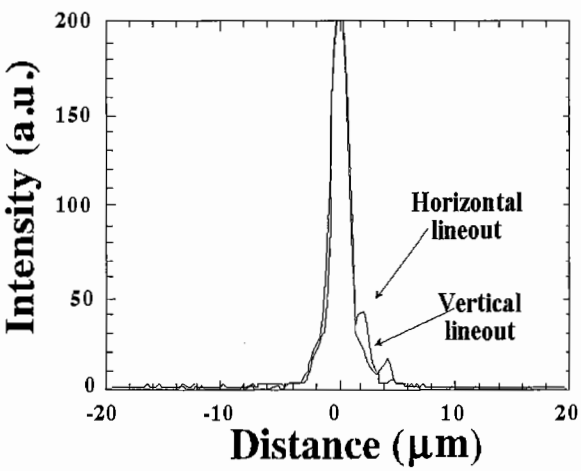

Fig. 6. Transverse 1D lineout of the focal spot (vertical and horizontal) of the low-energy compressed pulse (attenuated from 280 mJ) using an $F/2$ off-axis parabola. The 2.0 μm FWHM diameter focal spot is about 1.5 times diffraction–limited

5 Summary

We have observed that parasitic transverse lasing in large-aperture (> 3 cm) Ti:sapphire amplifiers can seriously impair their performance. Among the problems are limited extraction efficiency and restrictive timing requirements. Lower titanium concentrations and longer crystal lengths are preferred, since this helps avoid parasitic lasing. In addition, we have shown that suppression of the parasitics can be accomplished by careful index matching at the disk edges.

A new Ti:sapphire CPA laser system has been built which currently produces laser pulses with a duration of 75 fs centered at 800 nm, ≥ 15 J with a $\approx 1.5\times$ diffraction-limited focused spot size. These pulses can be generated at up to 3 per hour. To date, this is undoubtedly the highest-intensity laser ever demonstrated. The use of 100 fs class pulses in combination with high energy provides significant flexibility in not only focal intensity but also experimental geometry. For example, experiments can be performed in a high-aspect-ratio planar geometry while maintaining high peak intensity.

Initial target experiments seek to measure the photonuclear activation of gold. An analysis of the various isotopes produced will serve as an independent confirmation that peak intensities exceeding 10^{21} W/cm^2 have been achieved.

Acknowledgements. This research was performed under the auspices of the U.S. Department of Energy by Lawrence Livermore National Laboratory, under contract W-7405-Eng-48.

References

1. J.D. Bonlie, W.E. White, D.F. Price, D.H. Reitze: Proc. SPIE **312**, 2116 (1994)
2. J. Bonlie, D.F. Price, A. Sullivan, W.E. White: Proc. SPIE **107**, 2701 (1996)
3. A. Sullivan, J. Bonlie, D.F. Price, W.E. White: Opt. Lett. **21**, 603 (1996)
4. G.A. Mourou, C.P. Barty, M.D. Perry: Phys. Today **51**, 22 (1998)

5. W. Koechner: *Solid-State Laser Engineering*, 4th edn. (Springer-Verlag, Heidelberg, Germany 1996)
6. J.P. Chambaret, C. Le Blanc, G. Cheriaux, P. Curley, G. Darpentigny, P. Rousseau, G. Hamoniaux, A. Antonetti, F. Salin: Opt. Lett. **21**, 1921 (1996)
7. K. Yamakawa, M. Aoyama, S. Matsuoka, H. Takuma, C.P.J. Barty, D. Fittinghoff: Opt. Lett. **23**, 525 (1998)
8. A.E. Siegman: *Lasers* (University Science Books, Mill Valley, CA, USA 1986)
9. J.A. Britten, M.D. Perry, B.W. Shore, R.D. Boyd: Opt. Lett. **21**, 540 (1996)
10. R. Boyd, J.A. Britten, B.W. Shore, B. Stuart, M.D. Perry: Appl. Opt. **34**, 1697 (1995)
11. W.R. Sooy, R.S. Congleton, B.E. Dobratz, W.K. Ng: In Proc. Quantum Electron. Conf. 2, Paris, France, 1103 (1963)
12. J.B. Trenholme: Naval Research Laboratory, *Memorandum Report 2480* (1972)
13. J.E. Swain, R.E. Kidder, K. Pettipiece, F. Rainer, E.D. Baird, B. Loth: J. Appl. Phys. **40**, 3973 (1969)
14. S. Guch, Jr.: Appl. Opt. **15**, 1453 (1976)
15. H.T. Powell, M.O. Riley, C.R. Wolfe, R.E. Lyon, J.H. Campbell, E.S. Jessop, J.E. Murray: *Composite polymer–glass edge cladding for laser disks*, United States Patent 4849036 (1989)
16. J.M. Eggelston, L.G. DeShazer, K.W. Kangas: IEEE J. Quantum Electron. **QE-24**, 1009 (1988)
17. F.G. Patterson, J. Bonlie, D. Price, B. White: Opt. Lett. 24 **14**, 963 (1999)
18. P.F. Moulton: J. Opt. Soc. Am. B **3**, 125 (1986)
19. J. Itatani, J. Faure, M. Nantel, G. Mourou, S. Watanabe: Opt. Commun. **148**, 70 (1998)
20. W.E. White, F.G. Patterson, R.L. Combs, D.F. Price, R.L. Shepherd: Opt. Lett. **18**, 1343 (1993)
21. A. Sullivan, W.E. White: Opt. Lett. **20**, 192 (1995)
22. D.J. Kane, R. Trebino: Opt. Lett. **18**, 823 (1993)